Supporting Information

Choi and Puglisi 10.1073/pnas.1719592115

SI Materials and Methods

Measurement of R_0 Value for Cy5/QSY21 Pair. One biotinylated DNA oligonucleotide [5′-biotin-GCTTATTCAA CTACACTTCT CGGCCTC-(Cy5)-3′] and four cDNA oligonucleotides with varying length [5′-GAGGCCGAGA AGTGTAGT-(QSY21)-3′, 5′-GAGGCCGAGA AGTGTA-(QSY21)-3′, 5′-GAGGCCGAGA AGTG-(QSY21)-3′, and 5′-GAGGCCGAGA AG-(QSY21)-3′] were purchased from Trilink. Each cDNA oligonucleotide was annealed with the biotinylated DNA oligonucleotides by mixing them (10 μM of each oligo in 50 mM Tris-Acetate, pH 7.5, at 25 °C and 100 mM of potassium chloride), raising the temperature to 90 °C, and slow cooling them in a heat block to room temperature before the experiment. Each annealed DNA oligonucleotide mixture was immobilized in a separate channel of a quartz slide [machined as previously described (1)] via biotin–Neutravidin interactions. Measurement of the intensity of each immobilized Cy5/QSY21 molecule was measured using a custom prism-based total internal reflection fluorescence microscope as previously described, at 200 ms time resolution for 4 min, illuminated by the 632-nm laser at 0.10 mW·mm^{-2}. Distances (R) between Cy5 and QSY21 were calculated assuming a 3.4 Å distance per DNA base pair for each annealed DNA oligonucleotide. Given the FRET equation for quencher of $E_{FRET} = 1 - I_{quenched}/I_{unquenched} = 1/(1 + (R/R_0)^6)$, we could rearrange the equation to $I_{quenched} = I_{unquenched}(1 - 1/(1 + (R/R_0)^6))$, and fit five intensity measurements, mean intensities from four annealed products and one base DNA oligonucleotide, to estimate both $I_{quenched}$ and the R_0 value for Cy5/QSY21 pair and provide the 95% confidence interval as the specified error.

Reagents for Single-Molecule Experiments. Reagents and buffers were prepared as previously reported (1, 2). Briefly, each small and large subunit was mutated to include a weakly forming RNA hairpin at helix 44 and helix 101, which was used to attach Cy3B/QSY7 or Cy5/QSY21 labeled DNA oligonucleotides via RNA/DNA hybridization [DNA sequences for short oligonucleotides are: 5′-GAGGCCGAGA AGTG-(QSY21)-3′ and 5′-(Cy5)-GGGAGATCAG GATA-3′]. Elongator tRNAs (lysine-specific and phenylalanine-specific tRNA) were purchased from Sigma–Aldrich and labeled at the acp^{3}U47 position with Cy3, Cy5, or QSY9 using NHS chemistry as previously described (Cy3-NHS-ester and Cy5-NHS-ester were purchased from GE Healthcare, and QSY9-NHS-ester was purchased from ThermoFisher). Formyl-methionine–specific tRNA from Chemical Block Ltd. was labeled at the s^{4}U8 position using maleimide chemistry as previously described (Cy3-Maleimide was purchased from GE Healthcare). The synthetic Biotinylated RNA oligonucleotide used as mRNA was purchased from GE Dharmacon, with a 5′-UTR adapted from gene 32 of the T4 phage (5′-CAACCUAAAACUUACACACGCCCCGGUAAGGAAAUAAAA-3′), followed by the coding region [5′-AUG(UUCAAA)$_6$UAA(U)$_{12}$-3′], where the subscripted number signifies repeats. Translational factors, ribosomal S1 protein, and aminoacylated tRNAs were prepared as previously reported. EF-G was mutated to a single-cysteine form (C114D, C266A, C398S, and R637C) and labeled using Cy5-maleimide as previously described. The translocation activity of the double-cysteine mutated form (added D630C to R637C mutation) of EF-G has been published by Chen et al. (3).

Single-Molecule Experiments on a Zero-Mode Waveguide Instrument. Small and large ribosomal subunits were mixed with respective fluorescently labeled DNA oligonucleotide at 1:1.2 stoichiometric ratio with 1 μM final concentration of the subunit in the polymix buffer (50 mM Tris-acetate, pH 7.5, at 25 °C; 100 mM potassium chloride; 5 mM ammonium acetate; 0.5 mM calcium acetate; 5 mM magnesium acetate; 0.5 mM EDTA; 5 mM putrescine-HCl; and 1 mM spermidine) and incubated in the 37 °C water bath for 10 min, followed by incubation in the 30 °C water bath for 20 min. Afterward, the tube containing the large subunit was kept on ice, whereas the small subunit was incubated with S1 ribosomal protein at 1:1 stoichiometric ratio with 0.5 μM final concentration in the 37 °C water bath for 5 min because S1 ribosomal proteins may not have been copurified with the small subunit. Next, the small subunit was mixed with biotinylated mRNA, initiation factor 2, aminoacylated formyl-methionine tRNA at 1:2:13:4 with 150 nM final concentration of the small subunit in the polymix buffer, supplemented with 4 mM GTP, and incubated in the 37 °C water bath for 5 min, to form preinitiation complexes. Formed complex was diluted to 10 nM in polymix buffer (with different magnesium acetate concentration depending on the experimental conditions desired, ranging from 3.5 mM to 15 mM) supplemented with 4 mM GTP and the imaging mix [2.5 mM of PCA (protocatechuic acid), 2.5 mM of TSY, and 2× PCD (protocatechuate-3,4-dioxygenase), purchased from Pacific Bioscience (product number 100–228-700) and PCD added last)], and incubated in the zero-mode waveguide chip treated with Neutravidin at room temperature for 3 min, which binds to the Biotin-PEG (Polyethylene glycol) on the chip. After immobilizing preinitiation complex, the chip was washed three times using the same buffer without the complex to remove unbound complexes. At the same time, tRNA ternary complex was formed by incubating tRNA with 100 μM EF-Tu•GTP within the Buffer-6 (polymix buffer without spermidine and putrescine), supplemented with fresh 1 mM GTP, and incubated in the 37 °C water bath for 1 min. The delivery mix was formed in the polymix buffer (at desired magnesium acetate concentration) supplemented with 4 mM GTP, the imaging mix, 40/200 nM of (Phe/Lys) tRNA ternary complexes (labeled according to the experimental design), 80 nM of EF-G, and 200 nM of the large subunit and kept on the wet ice. For high-factor concentration experiments, tRNA ternary complex concentrations were increased to 300 nM, and EF-G concentrations were increased to 400 nM. Both the chip and the delivery mix were loaded onto the zero-mode waveguide instrument (RSII, purchased from Pacific Bioscience).

Detailed development and specification of the Pacific Bioscience RSII instrument as a platform for single-molecule fluorescence microscopy has been published previously (4). Fluorescence signals were recorded for 8 min with a frame rate of 10 frames per second after the delivery mix was delivered to the chip on the optical stage using robotic pipet, illuminated by 72 mW·mm^{-2} of 532-nm laser and 24 mW·mm^{-2} of 642-nm laser. Resulting movies were analyzed using in-house–written MATLAB (MathWorks) scripts, as previously described (4). Briefly, traces from each zero-mode waveguide well were filtered based on the presence of both fluorophores using automated scripts, and their expected correlation was checked and picked out manually. Our criteria involved two fluorescence signals at different time points; signals from fluorophores on surface-immobilized ribosomes were expected to be present at the beginning of the movie, whereas signals from fluorophores attached to tRNA and EF-G were expected not to be. This criterion, combined with tRNA binding and ribosome conformational changes,

has allowed picking actively translating molecules. E-site tRNA dissociation rates and state transition rates were annotated manually and calculated by fitting a single-exponential distribution to the measured state lifetimes using a maximum-likelihood estimation in MATLAB. For generating postsynchronized plots, each trace was preprocessed by subtracting low-intensity state fluorescence level (nonrotated state for the intersubunit rotation signal; tRNA absence state for the tRNA signal) first and normalizing all intensity over the high-intensity fluorescence state (preinitiation state for the intersubunit rotation signal; tRNA unquenched state for the tRNA signal). Experimental data represented in the supplementary figures are also provided in Dataset S1.

Thermodynamic Parameters of the Transition States. Similar to refs. 5 and 6, we have used Eyring equation to fit our data:

$$\ln(k) = -\frac{\Delta H^{\ddagger}}{R}\cdot\frac{1}{T} + \ln\left(\frac{k_B T}{h}\right) + \frac{\Delta S^{\ddagger}}{R},$$

where h, k_B, and R are Planck, Boltzmann, and universal gas constants, respectively. Next, the following Gibbs–Helmholtz equation was used to calculate $\Delta G^{\ddagger}$ from obtained parameters:

$$\Delta G^{\ddagger} = \Delta H^{\ddagger} - T\Delta S^{\ddagger}.$$

1. Blanchard SC, Gonzalez RL, Kim HD, Chu S, Puglisi JD (2004) tRNA selection and kinetic proofreading in translation. *Nat Struct Mol Biol* 11:1008–1014.
2. Aitken CE, Puglisi JD (2010) Following the intersubunit conformation of the ribosome during translation in real time. *Nat Struct Mol Biol* 17:793–800.
3. Chen C, et al. (2016) Elongation factor G initiates translocation through a power stroke. *Proc Natl Acad Sci USA* 113:7515–7520.
4. Chen J, et al. (2014) High-throughput platform for real-time monitoring of biological processes by multicolor single-molecule fluorescence. *Proc Natl Acad Sci USA* 111:664–669.
5. Steinert HS, Rinnenthal J, Schwalbe H (2012) Individual basepair stability of DNA and RNA studied by NMR-detected solvent exchange. *Biophys J* 102:2564–2574.
6. Rinnenthal J, Klinkert B, Narberhaus F, Schwalbe H (2010) Direct observation of the temperature-induced melting process of the Salmonella fourU RNA thermometer at base-pair resolution. *Nucleic Acids Res* 38:3834–3847.

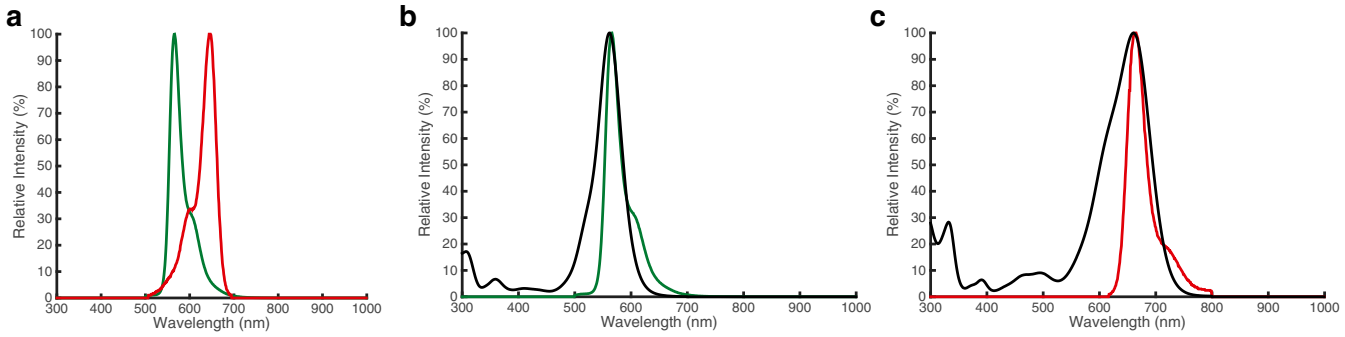

Fig. S1. Overlap of optical spectra for Cy3/Cy5, Cy3/QSY9, and Cy5/QSY21 smFRET pairs: (*A*) Cy3 emission (green) and Cy5 excitation (red) spectra. (*B*) Cy3 emission (green) and QSY9 absorption (black) spectra. (*C*) Cy5 emission (red) and QSY21 absorption (black) spectra. Data were provided by ThermoFisher.

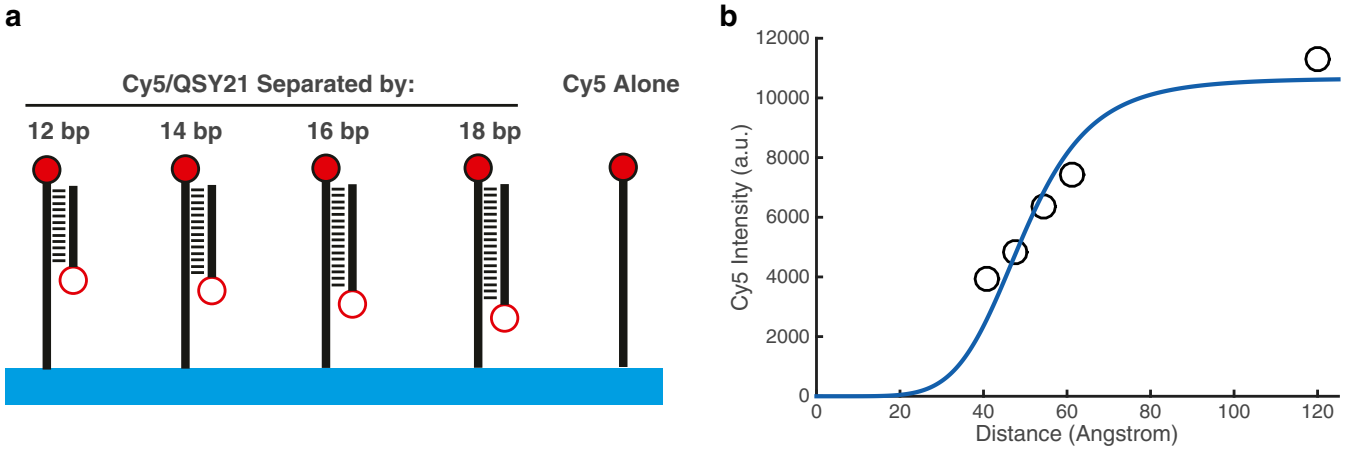

Fig. S2. Measured R_0 for the Cy5/QSY21 smFRET pair. (*A*) Experimental schematics for measuring Cy5/QSY21 quenching at different intermolecular distances. (*B*) Calculation of R_0 for Cy5/QSY21 smFRET pair, using measured mean Cy5 fluorescence intensity as a function of distance $[I_{\text{quenched}} = I_{\text{unquenched}}(1 - 1/(1 + (R/R_0)^6))]$. R-square value is 0.8958, $R_0 = 49.35$ (40.66, 58.04) Å, $I_{\text{unquenched}} = 10{,}700$ (7,500, 13,800), where values within parentheses show 95% confidence bound.

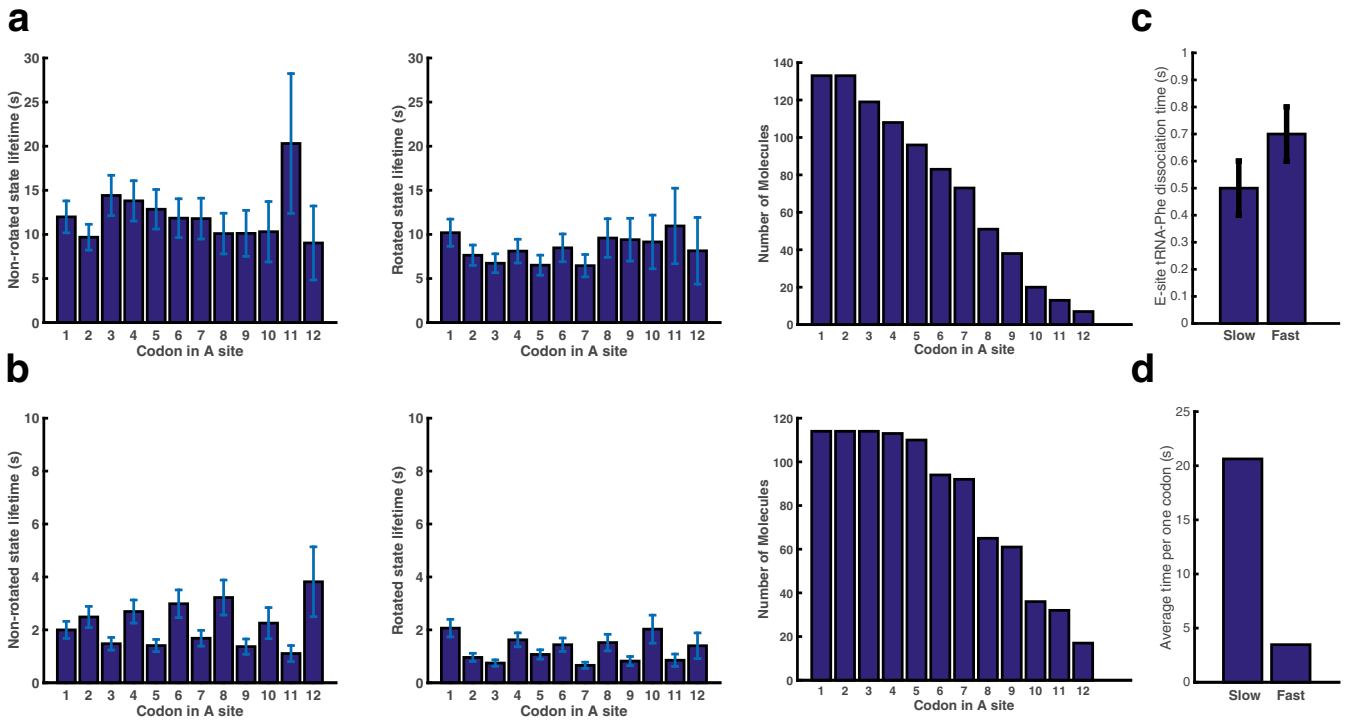

Fig. S3. Translation state lifetimes at two different factor conditions. (*A* and *B*) (*Left*) Nonrotated and (*Middle*) rotated state lifetimes per each codon and (*Right*) number of molecules translating each codon. (*A*) The 20 nM Phe-(QSY9)-tRNA^{Phe} and 100 nM Lys-(Cy3)-tRNA^{Lys}, and 40 nM EF-G (slow), and (*B*) 150 nM Phe-(QSY9)-tRNA^{Phe} and 150 nM Lys-(Cy3)-tRNA^{Lys}, and 200 nM EF-G (Fast) final concentration. (*C*) E-site (QSY9)-tRNA^{Phe} dissociation lifetime measured at two conditions ($n = 102$ and 197 for slow and fast conditions, respectively). (*D*) Average time to translate one codon (average of the sum of rotated and nonrotated state lifetimes at each codon).

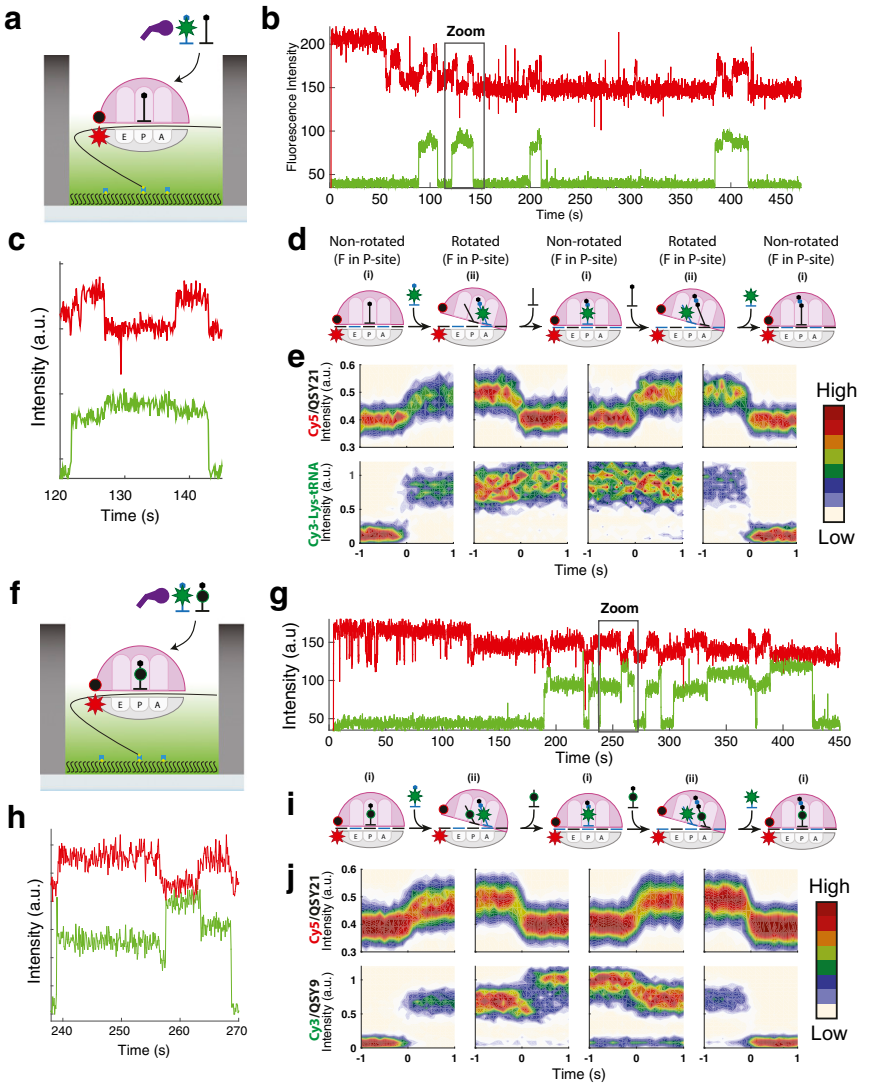

Fig. S4. Observing multiple translation–elongation cycles using two dye–quencher pairs. (*A–E*) An experiment with unlabeled Phe-tRNA^{Phe} to benchmark the Cy3 signal on tRNA. (*A*) An experimental schematic, including fluorescently labeled reagents used in *B–E*. (*B*) A representative experimental single-molecule trace. (*C*) Zoomed-in view of *B*, showing a slight Cy3 intensity change as tRNA transitions from the A/P to P to P/E sites, correlated with the Cy5 ribosomal conformational change signal. (*D*) Schematic for two translation–elongation cycles over two codons: nonrotated state (indicated by i) and rotated state (indicated by ii). (*E*) Postsynchronized plots of the (*Top*) Cy5/QSY21 ribosomal signal and (*Bottom*) Lys-(Cy3)-tRNA^{Lys} signal for each state transitions observed: Lys-(Cy3)-tRNA^{Lys} accommodation (first column), translocation (second column), Phe-tRNA^{Phe} accommodation (third column), and translocation (fourth column) (n = 176 and 166 for first and second columns and third and fourth columns, respectively). (*F–J*) An experiment with two dye–quencher pairs, same as in Fig. 1. (*F*) An experimental schematic, including involved labeled reagents for *G–J*. (*G*) A representative experimental trace. (*H*) Zoomed-in view of *G*. (*I*) Schematic for two translation–elongation cycles over two codons: nonrotated state (indicated by i) and rotated state (indicated by ii). (*J*) Postsynchronized plots of (*Top*) the Cy5/QSY21 ribosomal signal and (*Bottom*) the Cy3/QSY9 tRNA signal for each state transitions observed: Lys-(Cy3)-tRNA^{Lys} accommodation (first column), translocation (second column), Phe-tRNA^{phe} accommodation (third column), and translocation (fourth column) (n = 303 and 256 for first and second columns and third and fourth columns, respectively).

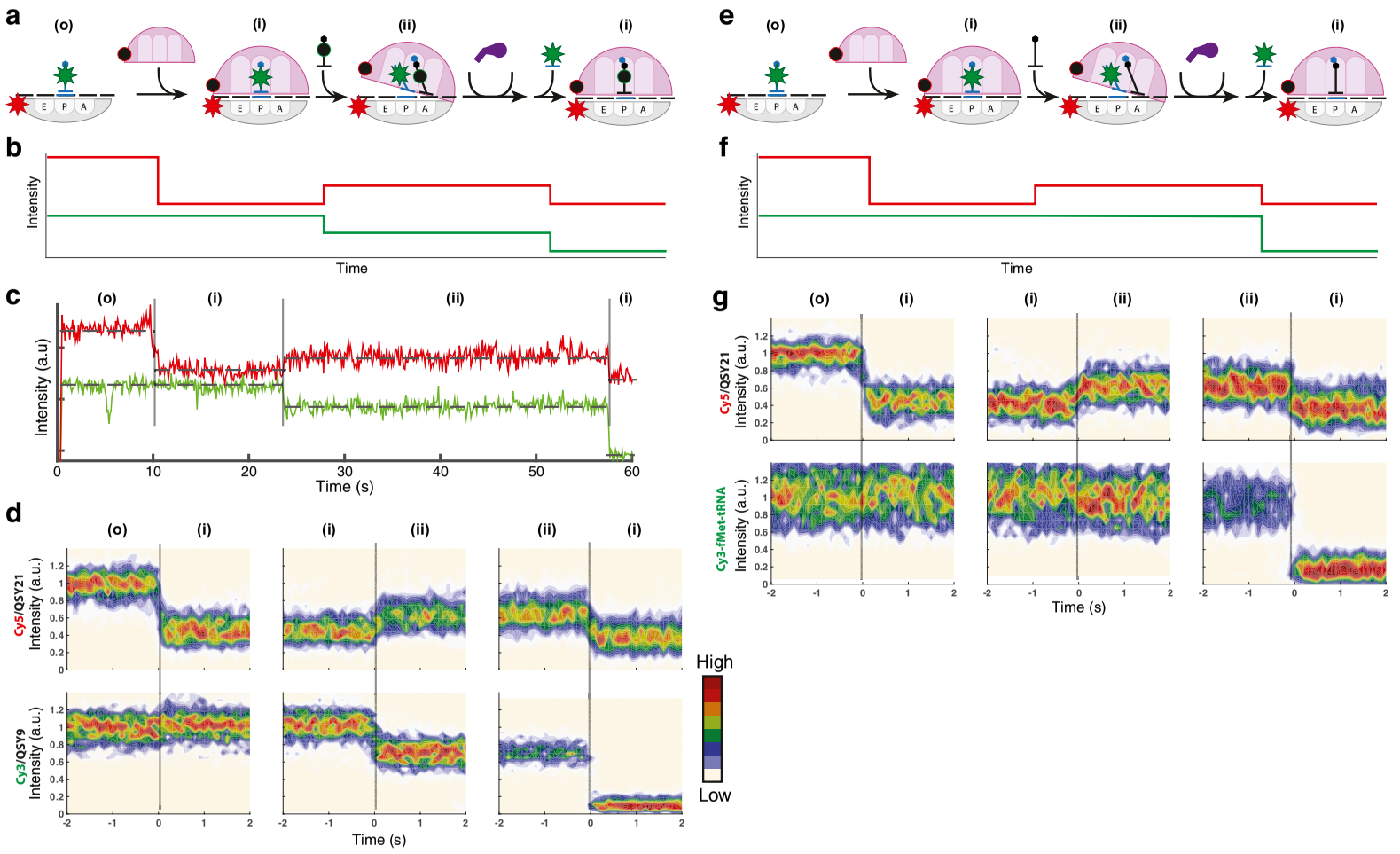

Fig. S5. Observing the first translation–elongation cycle using two dye–quencher pairs. (*A*) Schematic for the first translation–elongation cycle over one codon after initiation: o indicates preinitiation complex formed with mRNA, Cy5-30S, and Cy3-fMet-tRNA^{fMet}; i indicates nonrotated state after the QSY21-50S joins; and ii indicates rotated state after accommodation of (QSY9)-tRNA^{Phe} to the A site and peptidyl transfer reaction. (*B*) Expected sequence of Cy3 and Cy5/QSY21 signals for each state in *A*. (*C*) A representative experimental single-molecule trace of this experiment. (*D*) Postsynchronized plots of the Cy5/QSY21 signal (*Top*) and the Cy3/QSY9 signal (*Bottom*) for each state transitions observed: (*Left*) initiation, (*Middle*) tRNA accommodation, and (*Right*) translocation (n = 103). (*E–G*) Baseline intensity change of Cy3 attached to tRNA^{fMet} without the respective quencher (QSY9) attached to tRNA^{Phe}. (*E*) Schematic for the first translation–elongation cycle over one codon after initiation: o indicates preinitiation complex formed with mRNA, Cy5-30S, and Cy3-fMet-tRNA^{fMet}; i indicates nonrotated state after the QSY21 labeled large subunit joins; and ii indicates rotated state after accommodation of tRNA^{Phe} to the A site and peptidyl transfer reaction. (*F*) Expected sequence of Cy3 and Cy5/QSY21 signals for each state in *E*. (*G*) Postsynchronized plots of (*Top*) the Cy5/QSY21 signal and (*Bottom*) the Cy3 signal for each state transitions observed: (*Left*) initiation, (*Middle*) tRNA accommodation, and (*Right*) translocation, showing no quenching of Cy3 signal without its respective quencher, QSY9 (n = 93).

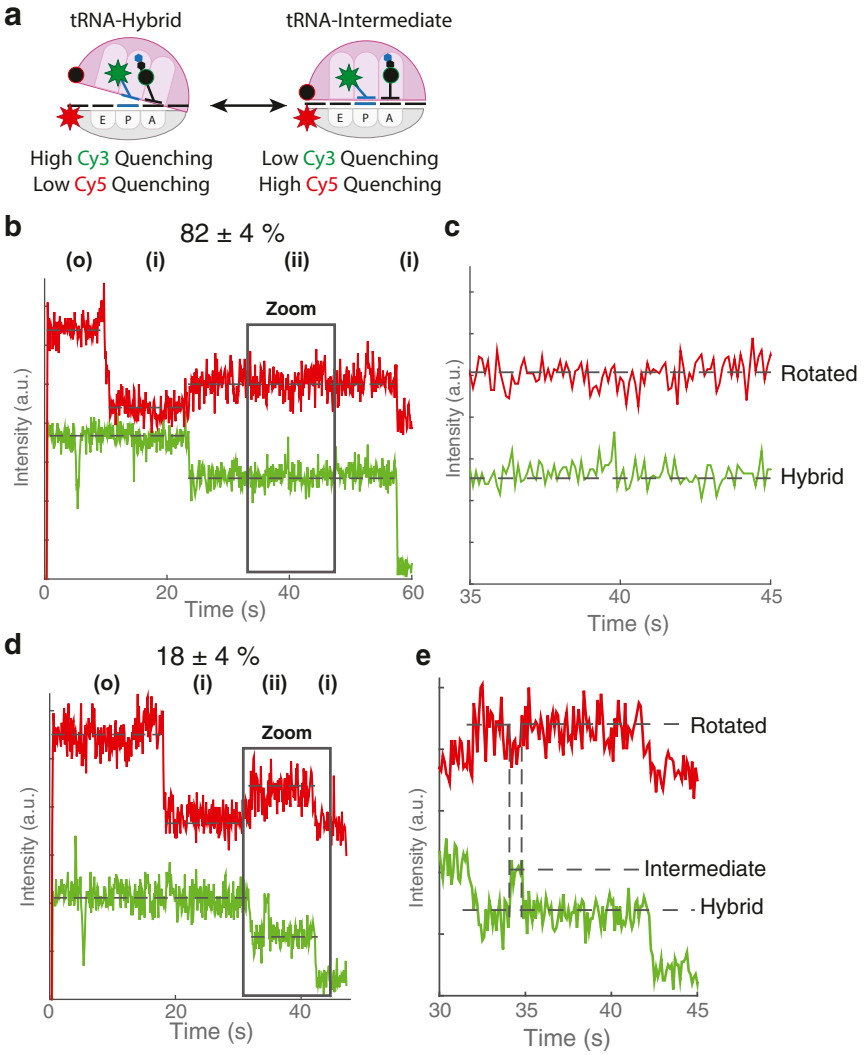

Fig. S6. Correlating two independent state transitions via dye–quencher pairs during the first round of the translation–elongation cycle. (*A*) An observed fluctuation between two substates within state ii, where the conformations of tRNAs [intermediate tRNA conformation, as observed by Munro et al. (1)] and ribosomes are coupled. (*B*) Representative experimental trace without coupled fluctuation. Eighty-two percent of traces did not show evidence of coupled fluctuation. (*C*) Zoomed-in view of *B* to show clearly the absence of a coupled fluctuation. (*D*) Representative experimental trace with observed coupled fluctuation. Eighteen percent of traces did show at least one coupled fluctuation between tRNA accommodation and translocation. (*E*) Zoomed-in view of *D* to show clearly a coupled fluctuation.

1. Munro JB, Altman RB, O'Connor N, Blanchard SC (2007) Identification of two distinct hybrid state intermediates on the ribosome. *Mol Cell* 25:505–517.

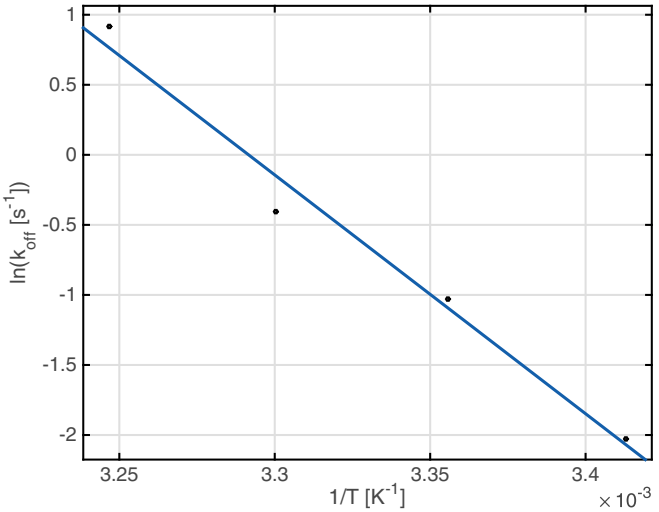

Fig. S7. Fitting data to the Eyring equation to estimate thermodynamics parameters for E-site tRNA dissociation. Numbers of instances used to determine each point are 158, 153, 210, and 212, from left to right on the plot (correspond to data from single experiments performed at 35, 30, 25, and 20 °C; corresponding data points are 7.6 ± 1.0, 2.8 ± 0.4, 1.5 ± 0.3, and 0.4 ± 0.1 s, where errors for each data point are from 95% confidence bounds of fitting data with single-exponential functions). R-square value is 0.9792, $\Delta H^{\ddagger} = 141.7$ (78.95, 204.5) kJ·mol^{-1}, and $\Delta S^{\ddagger} = 0.2218$ (0.0127, 0.4308) kJ·K^{-1}·mol^{-1}, where values within parentheses show 95% confidence bound of fitting Eyring equation to above four points. The error of temperature in each experiments are estimated to be ±1 °C, due to excitation laser heating of the sample chamber.

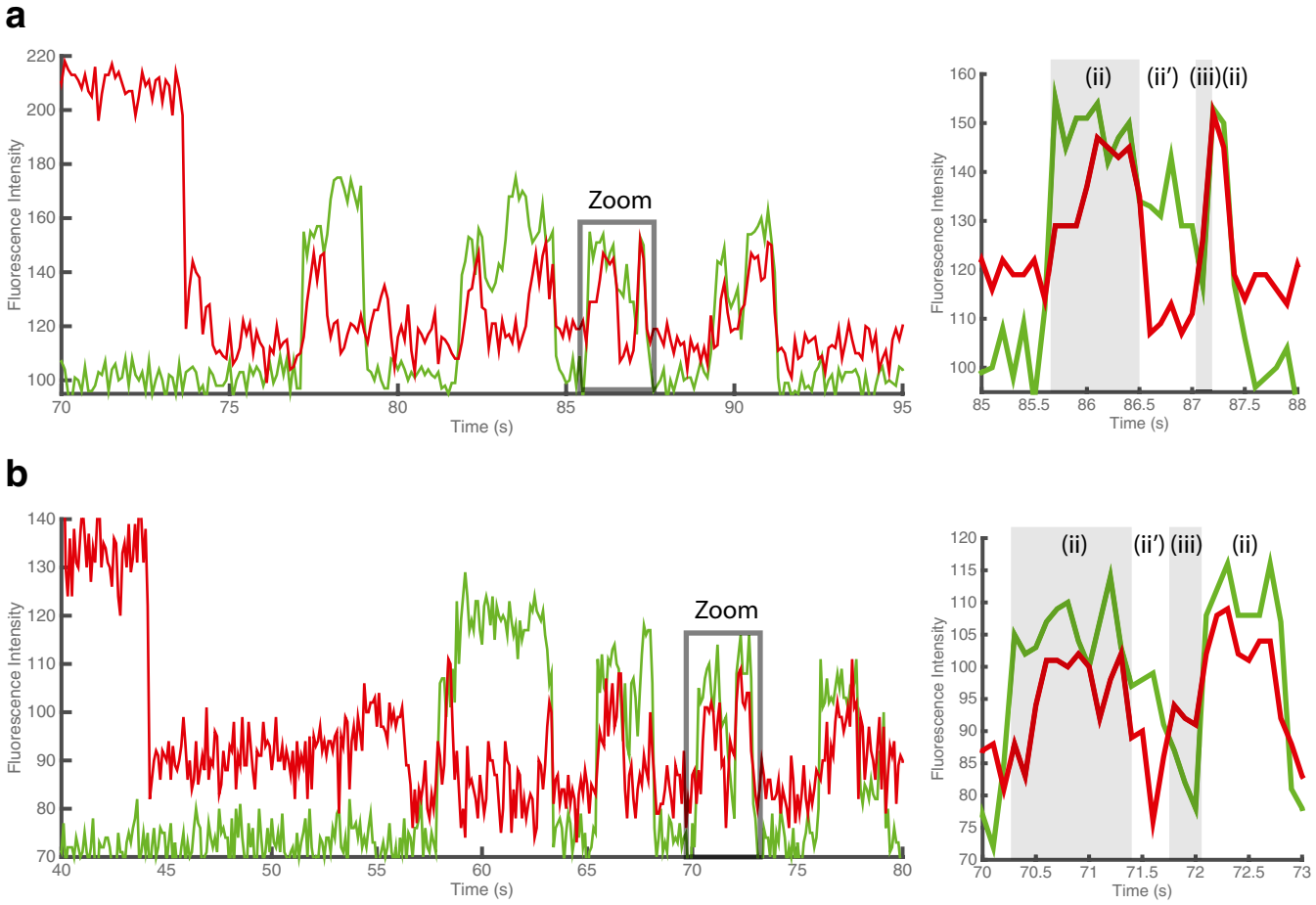

Fig. S8. Three-tRNA state observed under near-physiological conditions. At high factor concentrations [150 nM Phe-(QSY9)-tRNA^{Phe} and 150 nM Lys-(Cy3)-tRNA^{Lys}, and 200 nM EF-G], the partially rotated state is observed at near-physiological ionic strength (polymix buffer with 5 mM total Mg^{2+} concentration). (*A* and *B*) Representative traces from in vitro elongation at high factor concentrations and 5 mM Mg^{2+} condition.

Table S1. Estimated distances between dye–quencher pairs attached to the translational apparatus

Pair of labeling sites	Distance (Å)	PDB structure
Intersubunit (nonrotated)	35*	4V5G
Intersubunit (rotated)	47*	4V7D
tRNA–tRNA (classical)	38	4V5G
tRNA–tRNA (hybrid)	57	4V7D
tRNA(A/P)–EF-G	45	4V7D
tRNA(P/E)–EF-G	100	4V7D
tRNA(P)–tRNA(E)	44	4V5F
tRNA(P)–EF-G	50	4V5F

Due to the outward extension of ribosomal RNAs to place fluorophores and quenchers on the ribosome by dye-labeled DNA oligonucleotides/ribosomal RNA hybridization, distances specified for intersubunit labeling sites (marked by asterisks) may underestimate the real distances probed.

Other Supporting Information Files

Dataset S1 (XLSX)